

Digitally-Enhanced Wideband Analog-Digital Interfaces for Future Cognitive Radio Devices

Markus Allén, Jaakko Marttila and Mikko Valkama

Department of Communications Engineering

Tampere University of Technology

P.O. Box 553, FI-33101, Tampere, FINLAND

markus.allen@tut.fi, jaakko.marttila@tut.fi, mikko.e.valkama@tut.fi

Abstract—The cognitive radio concept has gained widespread interest to avoid spectral scarcity in next generation mobile communications systems. However, there are major challenges from the radio transceiver electronics point of view. This paper addresses the analog-to-digital converter saturation problem due to highly-varying signal conditions in wideband cognitive radio receivers. Two different post-processing approaches are proposed here to mitigate this nonlinear distortion. Their performance is compared to current state-of-the-art methods using laboratory radio signal measurements with commercially available hardware.

I. INTRODUCTION

Several recent studies have indicated that there are considerable temporal and spatial variations (i.e., inactivity) in the truly realized radio spectrum utilization [1]. This offers room for intelligent or cognitive radio (CR) devices, being able to sense the characteristics of their spectral environment and flexibly adapt their own radio waveforms, to communicate over the spatially and/or temporally unused spectral chunks as secondary users without affecting the licensed or primary operation. However, one major bottleneck related to the deployment of CR devices is the implementation of the needed radio transmitters and receivers [2]-[4]. The used radios should operate over extremely wide bandwidths, covering possibly several decades of radio spectrum as a whole, and be able to sense and communicate under extreme dynamic range conditions (possibly up to 100 dB). Especially for analog radio frequency (RF) modules and analog-digital (A/D) interfaces, the requirements on the sensitivity and linearity are essentially pushed way beyond the reach of state-of-the-art radio electronics [5], [6].

In a wideband receiver, with this kind of dynamics in the received signal, any nonlinearity in the receiver can be crucial from the weak signal point of view. The weak desired signal can be lost if, e.g., intermodulation distortion (IMD) from a strong blocking signal falls on this frequency band [1]. This is the main scenario discussed in this paper from the A/D con-

verter (ADC) nonlinearity point of view. The source of nonlinearity is here assumed to be waveform clipping in the input of the ADC of a radio receiver due to improper signal conditioning. This is a probable case in a wideband receiver, where multiple high-power blocking signals can be present causing large fluctuations in the instantaneous signal dynamics [7].

ADC nonidealities, and related mitigation methods, have been widely discussed in the current literature, but most of the proposed methods demand calibration or offline characterization [8]-[11], which is not usually feasible for mobile receivers. Clipping, as a phenomenon, also differs from the other nonlinearities because look-up table based compensation is not possible. This is because there is no information left about the original waveform behavior during clipping.

In Section II, this paper proposes an enhanced adaptive interference cancellation (E-AIC) method which is an online post-processing technique and thus appropriate for mobile devices. Compared to our earlier adaptive interference cancellation (AIC) method [12], [13], it requires an additional ADC but its performance is significantly better. The secondary ADC is allowed to have low resolution and thus it can be very low-cost. Notice that conceptually similar ideas of using alternate or additional analog signal branches have been proposed in [14] for receiver LNA and mixer linearization.

Section III, in turn, proposes a different kind of approach to mitigate clipping distortion by recovering the clipping waveform using interpolation. The proposed maximum selection interpolation (MSI) technique is partly based on the interpolation method proposed by T. Tomioka *et al.* [15]. However, the MSI performs better due to more optimized filter design, lower computational complexity and different kind of decision logic. In Section IV, all the discussed methods are compared using radio signal laboratory measurements with commercially available hardware. Finally, Section V concludes the paper.

II. ENHANCED ADAPTIVE INTERFERENCE CANCELLATION METHOD

In the A/D conversion context, the original AIC method for reducing nonlinear distortion was discussed in [12] and [13]. From the clipping distortion mitigation point of view, it has a limited performance due to the distorted reference signal. This problem is bypassed in the E-AIC method, which is proposed in this section.

This work was supported by the Academy of Finland (under the project “Understanding and Mitigation of Analog RF Impairments in Multiantenna Transmission Systems”), the Finnish Funding Agency for Technology and Innovation (Tekes, under the project “Advanced Techniques for RF Impairment Mitigation in Future Wireless Radio Systems”) and the Technology Industries of Finland Centennial Foundation.

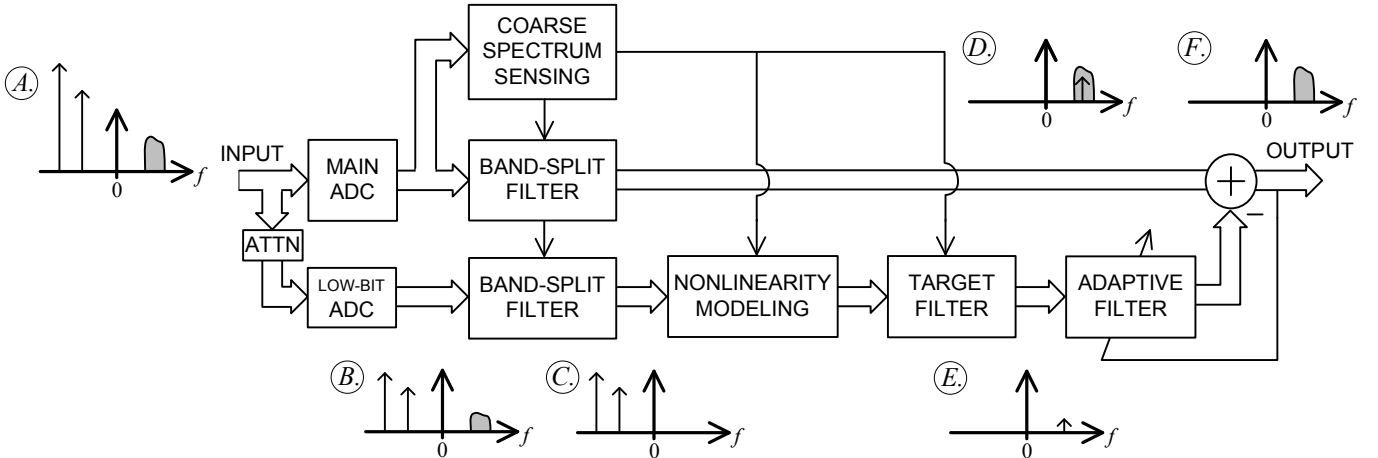


Fig. 1. Enhanced adaptive interference cancellation (E-AIC) method for reducing A/D converter clipping distortion at a weak signal band stemming from high-power blocking signals. Simplified spectra illustrate the processing flow using only a single intermodulation component as an example.

The working principle of E-AIC is illustrated in Fig. 1 with simplified spectrum examples. Due to improper input signal conditioning the received signal (see spectrum figure A) is unintentionally clipped in the main ADC and thus the IMD of the strong blocker signals is falling on top of the weak signal. The band-split filter removes the out-of-band spectral content and the distorted weak signal is shown in spectrum D (for simplification only a single IMD component is shown here). Concurrently, the input signal is digitized with a low-bit ADC using proper attenuation to prevent clipping (see spectrum B). Here only the strongest blocking signals are of interest to create an accurate reference signal for interference cancellation. The band-split filter preserves only the signal content outside the weak signal band as shown in spectrum C. The purpose of the nonlinearity modeling block is to regenerate the IMD present in the weak signal band based on the polynomial model of the form

$$s_{\text{ref}} = c_3 s_{\text{ref}}^3 + c_5 s_{\text{ref}}^5 + \dots \quad (1)$$

where s_{ref} and \hat{s}_{ref} are the reference signal before and after the nonlinearity modeling, respectively. Equation (1) is assuming zero-symmetric clipping, but non-symmetric clipping (contains DC offset prior to clipping) can be taken into account by adding also even powers to the model. After the modeling stage, the target filter is used to select only the distortion located at the weak signal band (see spectrum E). The coefficients c_3, c_5, \dots are found using an adaptive filter, which can be implemented, e.g., using the LMS algorithm. After that, the regenerated distortion is subtracted from the weak signal in order to remove the clipping-induced intermodulation distortion. The compensated signal without the distortion is illustrated in spectrum F.

The coarse spectrum sensing block in Fig. 1 represents the outer-loop control mechanism which manages the nonlinearity modeling stage and all the filters according to the locations of the most sensitive frequency bands. The required location information can be acquired rather straightforwardly in frequency domain. This functionality brings additional flexibility to the proposed compensation technique and actually it is a fundamental requirement in cognitive radio solutions.

III. CLIPPING COMPENSATION USING INTERPOLATION

In a digitized waveform all the clipped samples can be thought as lost samples and interpolation is one way to replace those with better estimates. Fig. 2 (a) illustrates a waveform after oversampling A/D conversion. Due to the oversampling the waveform can be represented as a polyphase decomposition which is shown in Fig. 2 (a) using different colors and symbols for samples in different polyphase branches. The fundamental idea behind the proposed interpolation method is based on the fact that the subsequent samples in the oversampled waveform contain redundant information, i.e., a clipped sample in one polyphase branch can be recovered based on the corresponding samples in other branches using a proper fractional delay filter. In Fig. 2 (a) this would mean that we can recover the clipped samples in Branch 1 using samples in Branches 2, 3 and 4.

The block diagram of the proposed MSI method is shown in Fig. 2 (b). After the oversampling A/D conversion the polyphase decomposition is formed. Unclipped samples can be passed through intact meaning that they are filtered with a filter corresponding to a pure delay. When there is a clipped sample in one polyphase branch, the other branches provide estimates to replace the clipped sample. After that, the decision logic chooses the estimate that has the largest absolute value and the chosen estimate replaces the clipped sample in the oversampled waveform. This overall procedure inside the interpolation processing block (see the gray box in Fig. 2 (b)) can be iterated several times to achieve more accurate results. The iteration essentially means that more and more information about the clipped sample is extracted from the other samples. This is stemming from the fact that usually there are clipped samples involved in the estimation calculation meaning that the estimate is not perfect. However, in the next iteration round we have better estimates for all the clipped samples involved in calculating new estimates. After all the interpolation processing is carried out, the enhanced signal is downsampled as shown in Fig. 2 (b).

In the proposed MSI method, the polyphase branch filters are formed by first designing a low-pass FIR filter of which pass-band corresponds to the non-oversampled signal band-

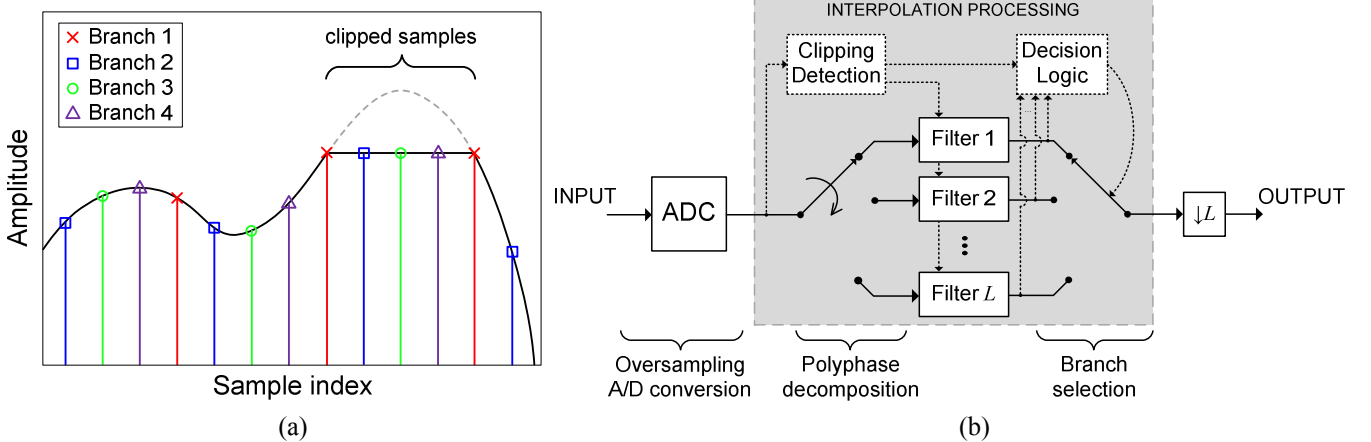


Fig. 2. (a) Illustration of a clipped waveform with oversampling factor of 4. Each polyphase branch has been depicted with different symbol and color. (b) Block diagram of the proposed maximum selection interpolation (MSI) method. A/D converter samples the input L times the rate of the final desired sampling rate. Polyphase filters provide estimates for a clipped sample and the decision logic chooses the estimate which has the highest absolute value to replace the clipped sample.

width, i.e., the normalized bandwidth of the pass-band is $1/L$, where L is the oversampling factor. If the overall impulse response is $h(n)$, the branch filters are

$$\begin{aligned} h_0(n) &= \{h(0), h(L), h(2L), \dots\} \\ h_1(n) &= \{h(1), h(L+1), h(2L+1), \dots\} \\ &\vdots \\ h_{L-1}(n) &= \{h(L-1), h(2L-1), h(3L-1), \dots\}. \end{aligned} \quad (2)$$

The clipping detection box in Fig. 2 (b) is responsible for assigning right impulse response for every polyphase branch. The assignment depends on the location of the clipped sample, i.e., the filter $h_0(n)$ should be always in the branch where the current clipped sample is. For example, if the clipped sample is in the second branch, the Filters 1, 2, ..., L in Fig. 2 (b) would be $h_{L-1}(n), h_0(n), h_1(n), \dots, h_{L-2}(n)$, respectively.

IV. MEASUREMENT RESULTS

This Section provides performance results from laboratory radio signal measurements using a commercial 14-bit ADC [16] and post-processing methods implemented in software. Both E-AIC and MSI methods are applied to the same test signal to obtain comparable results. In addition, performance of our original AIC method [12], [13] and Tomioka's interpolation technique [15] are given as a reference. Due to the limited amount of hardware reserved for the measurements, the low-bit ADC in E-AIC method is realized with the same 14-bit ADC and then the resolution is reduced by software.

The used test signal before and after clipping is illustrated in Fig. 3 both in time and frequency domain. It consists of five separate frequency bands with different bandwidths and power levels the overall dynamic range being in the order of 45 dB as a practical example case. The peak-to-average power ratio (PAPR) of the test signal is 7 dB before clipping and the sampling rate is 64 MHz for I and Q branches. Clipping level of 6 dB over the average power level of the test signal is chosen in Fig. 3 to demonstrate clipping phenomenon in time and frequency domain. Especially the strong blocker at -1 MHz is

causing third order IMD to the weak signal band around +3 MHz which is considered to be the band of interest.

The performances of the post-processing methods are compared using signal-to-noise-and-distortion ratio (SNDR) gain as a figure-of-merit. The SNDR gain is defined as a relation of SNDRs of the weak signal band (around +3 MHz) before and after applying the post-processing method. The results with different clipping levels are shown in Fig. 4. Four iteration rounds were performed for interpolation techniques (MSI and Tomioka) using 32-tap polyphase branch filters to achieve the presented results. The proposed MSI method is clearly performing better although its complexity is smaller than Tomioka's. This is because MSI doesn't require the preliminary polynomial interpolation stage used in Tomioka's method (see [15] for details). In addition, MSI employs a properly designed FIR filter whereas Tomioka's method uses a truncated sinc function. From the performance point of view, also the decision logic for branch selection has a great effect. However, the performance of both interpolation methods is limited due to other ADC nonidealities which affect the estimation accuracy.

In AIC and E-AIC methods third, fifth and seventh order nonlinearities were modeled to obtain the results in Fig. 4. Both are performing better than the interpolation techniques, because AIC and E-AIC are able to remove any kind of nonlinear distortion regardless of its source (like mixer and LNA nonlinearities in practice) whereas the interpolation can only consider the clipping distortion. The proposed E-AIC method is almost able to reach the ideal AIC performance level when a 7-bit secondary ADC is used with 7-dB input attenuation. Here the ideal AIC means that third, fifth and seventh order nonlinear distortion is removed using a perfect reference signal. The low SNDR gain with clipping levels 8-10 dB can be explained with the fact that there is not much distortion to remove at first place due to very mild clipping. Other reasons for the limited performance gains are inaccuracies in the nonlinearity modeling as well as in adaptive filter coefficients.

V. CONCLUSIONS

This paper focused on the saturation problem of ADCs stemming from highly-varying signal dynamics in wideband cognitive radio receivers. Two post-processing techniques were proposed to compensate the nonlinear distortion in a clipped signal. Their performance were verified using laboratory radio signal measurements and both the techniques showed significant improvement in performance compared to the current state-of-the-art methods in the literature.

REFERENCES

- [1] J. Yang, R. W. Brodersen and D. Tse, "Addressing the dynamic range problem in cognitive radios," in *Proc. IEEE Int. Conf. Communications (ICC-07)*, Glasgow, Scotland, June 2007, pp. 5183-5188.
- [2] B. Razavi, "Challenges in the design of cognitive radios," in *Proc. IEEE Custom Integrated Circuits Conf. (CICC-09)*, San Jose, CA, Sept. 2009, pp. 391-398.
- [3] D. Cabric, "Addressing feasibility of cognitive radios," *IEEE Signal Processing Mag.*, vol. 25, no. 6, pp. 85-93, Nov. 2008.
- [4] P.-I. Mak, S.-P. U, and R. P. Martins, "Transceiver architecture selection: review, state-of-the-art survey and case study", *IEEE Circuits and Systems Mag.*, vol. 7, 2nd quarter 2007, pp. 6-25.
- [5] B. Le, T. W. Rondeau, J. H. Reed and C. W. Bostian, "Analog-to-digital converters," *IEEE Signal Processing Mag.*, vol. 22, no. 6, pp. 69-77, Nov. 2005.
- [6] A. Rusu, D. Rodriguez de Llera Gonzalez and M. Ismail, "Reconfigurable ADCs enable smart radios for 4G wireless connectivity," *IEEE Circuits Devices Mag.*, vol. 22, no. 3, pp. 6-11, May-June 2006.
- [7] C. Svensson, "The blocker challenge when implementing software defined radio receiver RF frontends," *Analog Integrated Circuits and Signal Processing*, Dec. 2009.
- [8] P. Arpaia, P. Daponte and S. Rapuano, "A state of the art on ADC modeling," *Elsevier J. Computer Standards & Interfaces*, vol. 26, no. 1, pp. 31-42, Jan. 2004.
- [9] N. Björsell and P. Hänel, "Dynamic behavior models of analog to digital converters aimed for post-correction in wideband applications," in *XVIII Imeko World Congress 11th Workshop on ADC Modelling and Testing*, Rio de Janeiro, Brazil, 2006.
- [10] L. De Vito, H. Lundin and S. Rapuano, "Bayesian calibration of a lookup table for ADC error correction," *IEEE Trans. Instrum. Meas.*, vol. 56, no. 3, pp. 873-878, June 2007.
- [11] P. Arpaia, L. Michaeli and S. Rapuano, "Model-based compensation of SAR nonlinearity," *IEEE Trans. Instrum. Meas.*, vol. 58, no. 3, pp. 541-550, March 2009.
- [12] M. Allén, J. Marttila and M. Valkama, "Digital post-processing for reducing A/D converter nonlinear distortion in wideband radio receivers," in *Proc. Forty-Third Asilomar Conf. Signals, Syst., and Computers*, Pacific Grove, CA, Nov. 2009.
- [13] M. Allén, J. Marttila and M. Valkama, "Modeling and mitigation of nonlinear distortion in wideband A/D converters for cognitive radio receivers," *European Microwave Assoc. Int. J. Microwave and Wireless Technologies*, April 2010.
- [14] E. A. Keehr and A. Hajimiri, "Equalization of third-order intermodulation products in wideband direct conversion receivers," *IEEE J. Solid-State Circuits*, vol. 43, no. 12, pp. 2853-2867, Dec. 2008.
- [15] T. Tomioka, R. Sakata, T. Horiguchi, T. Tomizawa and K. Inoue, "A/D converter clipping noise suppression for high-sensitivity carrier-sensing of cognitive radio transceiver," in *IEEE Global Telecommunications Conference (GLOBECOM'07)*, Washington, DC, Nov. 2007.
- [16] Analog Devices, *AD9248 Data Sheet*, rev. A, March 2005. Available online at <http://www.analog.com/>

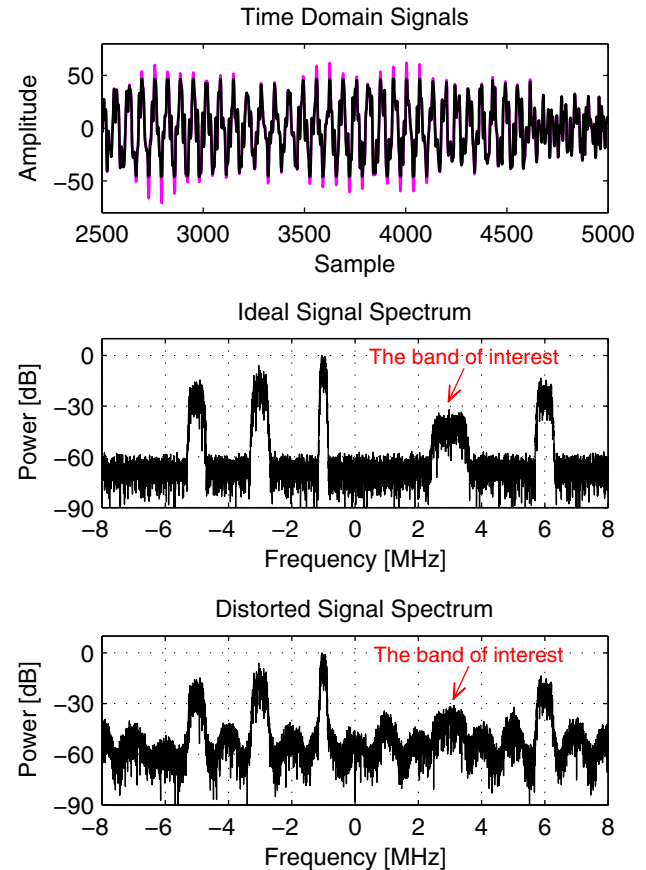


Fig. 3. Upper part: digitized waveform in time domain with and without clipping. Middle part: the unclipped waveform in frequency domain. Lower part: the clipped waveform in frequency domain illustrating the third-order intermodulation distortion at the weak signal around +3 MHz originating from the signal at -1 MHz. This laboratory measurement was carried out using 14-bit A/D converter clipping level being 6 dB over the average power level of the signal.

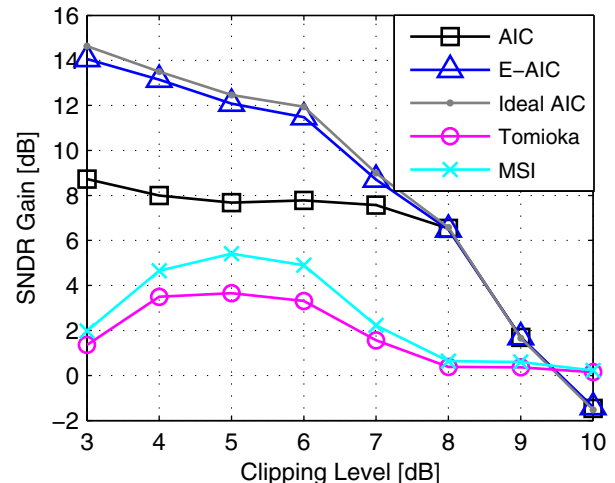


Fig. 4. SNDR gain comparison between different clipping compensation techniques. Clipping level is described as a number of dBs above the average power level of the signal.